

# THE X-RAY BEAM IMAGER FOR TRANSVERSAL PROFILING OF LOW-EMITTANCE ELECTRON BEAM AT THE SPRING-8

S. Takano\*, M. Masaki, and H. Ohkuma

Japan Synchrotron Radiation Research Institute, SPring-8, Hyogo 679-5198, Japan

## Abstract

The X-ray beam imager (XBI) at the accelerator diagnostics beamline I of the SPring-8 is briefly described. It has been developed for transversal profiling of the electron beam of the SPring-8 storage ring. It comprises a single Fresnel zone plate (FZP) and an X-ray zooming tube (XZT). The spatial resolution is 4  $\mu\text{m}$  ( $1\sigma$ ), and the time resolution is 1 ms. The field of view is vignetting-free and is larger than  $\phi 1.5$  mm. With the XBI, we have successfully observed the profiles of the electron beam having vertical emittance smaller than 10  $\text{pm}\cdot\text{rad}$ .

## INTRODUCTION

The SPring-8 is a third generation synchrotron light source operating since 1997. To observe the transverse profiles of the electron beam of the 8 GeV storage ring, we planned the XBI [1]. Our goal is the emittance diagnostics of the SPring-8 with resolution better than 1  $\text{pm}\cdot\text{rad}$ . The design targets of the XBI are 1) spatial resolution ( $1\sigma$ ) in the micron range, 2) time resolution of 1 ms, and 3) vignetting-free field of view larger than  $\phi 1$  mm on the coordinates of the electron beam. We have constructed the XBI at the accelerator diagnostics

beamline I (BL38B2) of the SPring-8 storage ring. The details of the XBI and the results of the measurements will be described elsewhere [2]. In this paper, we give brief descriptions of the XBI and some of the results obtained.

## THE X-RAY BEAM IMAGER (XBI)

The schematic layout of the diagnostics beamline I is shown in Fig.1. It has a bending magnet light source with an critical photon energy of 28.9 keV. The optical system of the XBI is shown in Fig.2. All the components of the XBI are in the optics hutch of the beamline. The XBI is based on a single FZP and an XZT. An X-ray image of the electron beam moving in the bending magnet is obtained by the FZP. To avoid the effect of the chromatic aberration of the FZP, monochromatic X-rays are selected by the double crystal monochromator. A 4-jaw slit is used to determine the horizontal width of the white X-ray beam incident on the monochromator to avoid unwanted heat load to the crystals. The magnification factor of the FZP is 0.274. We use an XZT to enlarge the reduced X-ray image of the electron beam. The observing photon energy of the XBI is 8.2 keV, which was determined by considering the

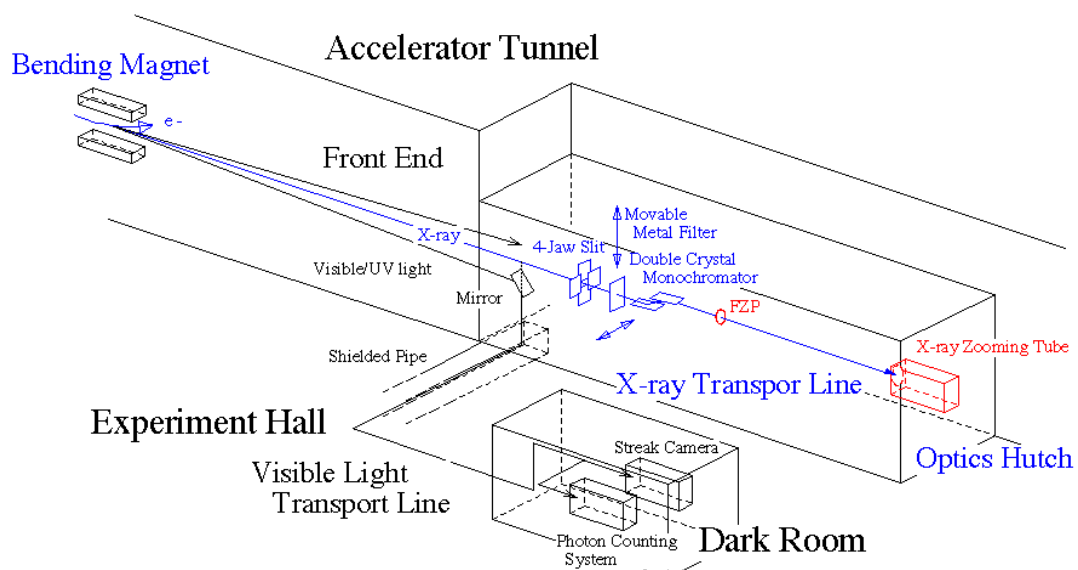


Figure 1: Layout of the SPring-8 accelerator diagnostics beamline I (BL38B2).

\* Email: takano@spring8.or.jp

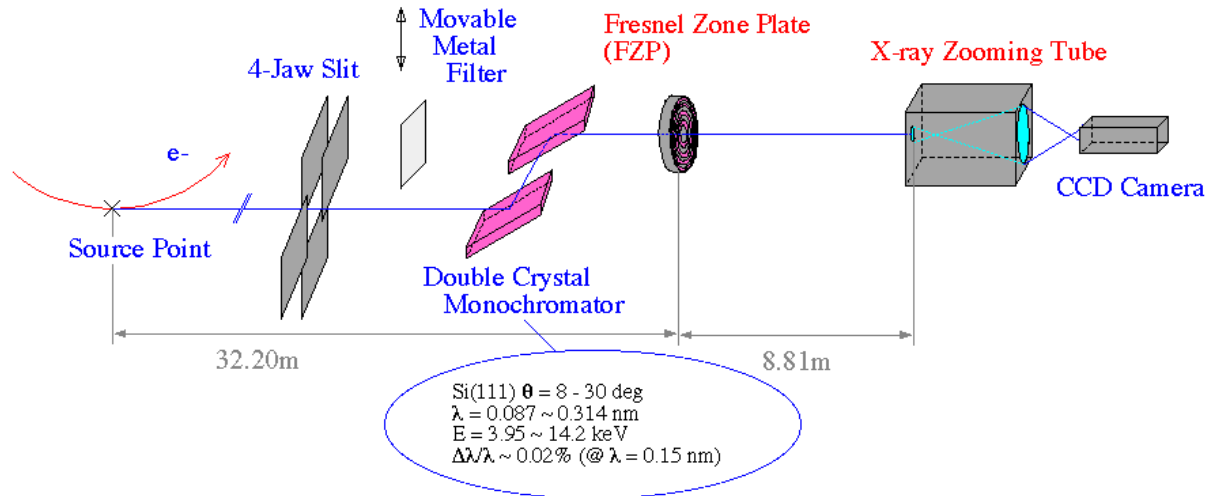


Figure 2: The optical system of the X-ray beam imager (XBI).

spatial resolution and the efficiencies of the FZP and the XZT.

The FZP was fabricated by NTT Advanced Technology Co. The characteristics of the FZP are summarized in Table 1. The width of the outermost zone is  $0.75 \mu\text{m}$ . An FZP with such wide outer zones can be fabricated without difficulties by the existing technologies and promises to achieve theoretical diffraction-limited resolution.

Table 1: Parameters of the FZP

Distance from the source point	32.20 m
Diameter	1.4 mm
Focal length *	6.92 m
Total number of zones	468
Outermost zone width	$0.75 \mu\text{m}$
Material of absorbing zones	Tantalum ( $2.0 \mu\text{m}$ thick)
Diffraction Efficiency *	32 %
Magnification factor	0.274
Spatial Resolution ( $1\sigma$ ) * $\sigma_{FZP}$	$1.5 \mu\text{m}$

\* Theoretical Value at  $E = 8.2 \text{ keV}$  ( $\lambda = 0.15 \text{ nm}$ ).

The XZT (Hamamatsu Photonics K. K., V4410) is a device which transforms an X-ray image on the input photocathode to a magnified visible light image on the output phosphor screen. The characteristics of the XZT are summarized in Table 2. We set the magnification at 50 for beam profile measurements. The response time of the XZT is predominated by that of the output screen. We have selected the P-47 phosphor as the screen material, because it has a fast decay time of 100 ns (from 100 % to 10 %). The contribution  $\sigma_{XZT}$  of the XZT to the spatial resolution of the XBI was determined to be  $3.8 \mu\text{m}$  experimentally [1]. To avoid degradation of the input photocathode of the XZT caused by exposure to

Table 2: Parameters of the XZT

Distance from the source point *	41.01 m
Input photocathode	Cesium iodide ( $0.3 \mu\text{m}$ thick)
Output screen	P-47 phosphor
Magnification factor #	50
Spatial Resolution ( $1\sigma$ ) & $\sigma_{XZT}$	$3.8 \mu\text{m}$

\* The value on the input photocathode.

# The values set at the beam profile measurements.

& Contribution to the XBI determined experimentally.

intense X-ray beams, we use a metal filter made of aluminum foil when the beam current is larger than 10 mA.

The output image of the electron beam from the XZT is observed by a CCD camera (Hamamatsu Photonics K. K., C4742-95). It has an effective area of  $8.6\text{mm}$  by  $6.9\text{mm}$  in  $1280 \times 1024$  pixels, and the corresponding field of view of the XBI is  $1.9 \text{ mm}$  by  $1.5 \text{ mm}$ , which is larger than the design target of  $\phi 1.0 \text{ mm}$ . The exposure time of the CCD camera can be changed in a range from  $0.1 \text{ ms}$  to  $10 \text{ s}$  by an electric shutter. The time resolution of the XBI is at present limited to be  $1 \text{ ms}$  by the maximum allowable photon flux density on the photocathode of the XZT.

## RESULTS

An example of the beam image of the SPring-8 observed with the XBI is shown in Fig. 3. The corresponding horizontal and vertical beam profiles are shown in Fig. 4. The optics of the ring was the so-called low-emittance optics introduced in 2002 [3]. The filling pattern of the ring consisted of 1920 bunches in equally spaced twelve trains of consecutive 160 bunches. The total beam current and the current of each bunch were 10

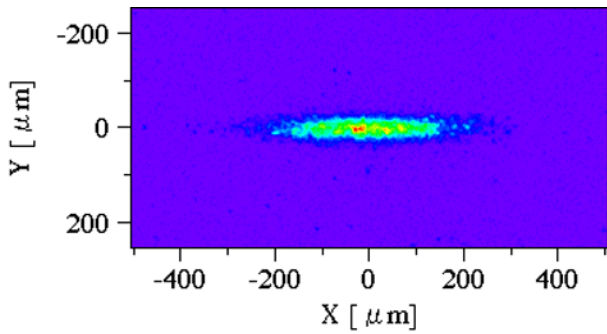


Figure 3: An example of the profile of the electron beam of the SPring-8 storage ring observed with the XBI

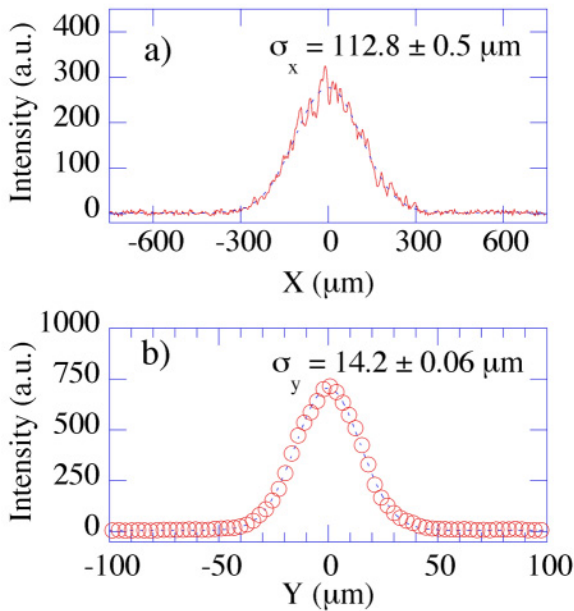


Figure 4: Horizontal and vertical beam profiles observed with the XBI with fitted Gaussian curves (dashed curves).

mA and 5  $\mu$ A, respectively. The magnet gaps of all the insertion devices were fully opened in to minimize the effects on the beam emittance. No metal filter was used, and the exposure time of the CCD camera was 1 ms. The horizontal and vertical beam sizes were  $\sigma_x = 112.8 \pm 0.5 \mu\text{m}$ , and  $\sigma_y = 14.21 \pm 0.06 \mu\text{m}$ , respectively, after subtraction of the spatial resolution of the XBI contributed by  $\sigma_{FZP}$  and  $\sigma_{XZP}$ . The errors denote statistical  $1\sigma$  fluctuations in successive measurements and not including systematic errors.

By using the design values of the betatron and the dispersion functions at the source point and the beam energy spread, we deduced the beam emittances from the beam sizes measured with the XBI. The horizontal and the vertical emittances were  $3.29 \pm 0.05 \text{ nm}\cdot\text{rad}$ ,  $7.26 \pm 0.06 \text{ pm}\cdot\text{rad}$ , respectively. The deduced horizontal emittance is consistent with the design value of 3.4 by taking a  $2\sigma$  statistical error. The deduced vertical

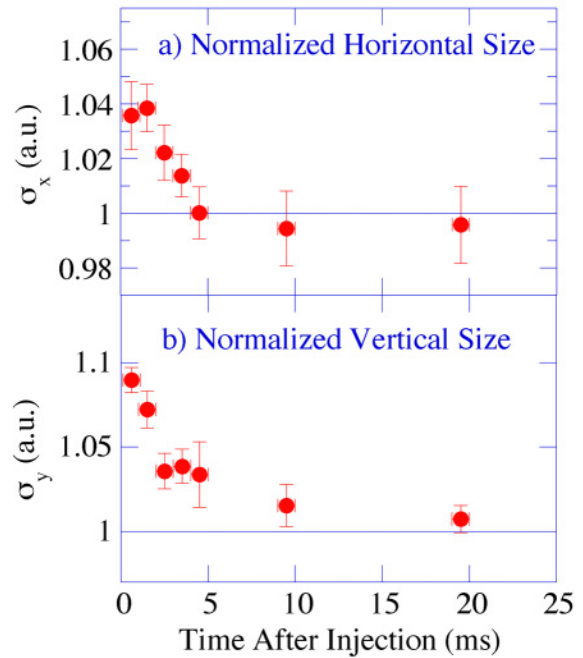


Figure 5: Effective beam sizes as functions of time after injections observed in the top-up operation.

emittance is smaller than  $10 \text{ pm}\cdot\text{rad}$ .

By utilizing the 1 ms time resolution of the XBI, we studied transient behaviors of the effective beam profile after beam injections in the top-up operation [4]. Fig. 5 shows observed time variation of the effective horizontal and vertical beam sizes normalized to those of the unperturbed stored beam. Small but significant increase of beam sizes were found after injections, but they return to the values of the unperturbed beam in a period shorter than injection intervals. It seems that the observed change of the beam sizes induced by injections are tolerable for most user experiments.

### FUTURE STEPS

Calibration of the point-spread function of the XBI is necessary to further improve the accuracies of the size measurements. For continuous monitoring of the beam profile, development of a real-time data acquisition system is planned.

### REFERENCES

- [1] S. Takano et al, DIPAC'01, Grenoble, 2001, p.145.
- [2] S. Takano et al, submitted to Nucl. Instr. and Meth. A.
- [3] M. Takao et. al., "Progress toward Brightness Improvements at the SPring-8 Storage Ring", APAC'04, Gyeongju, in the press.
- [4] H. Tanaka, et al., EPAC'04, Lucerne, 2004, p.222.